Supplementary Information

Section 1. Temperature of vapour phase detection

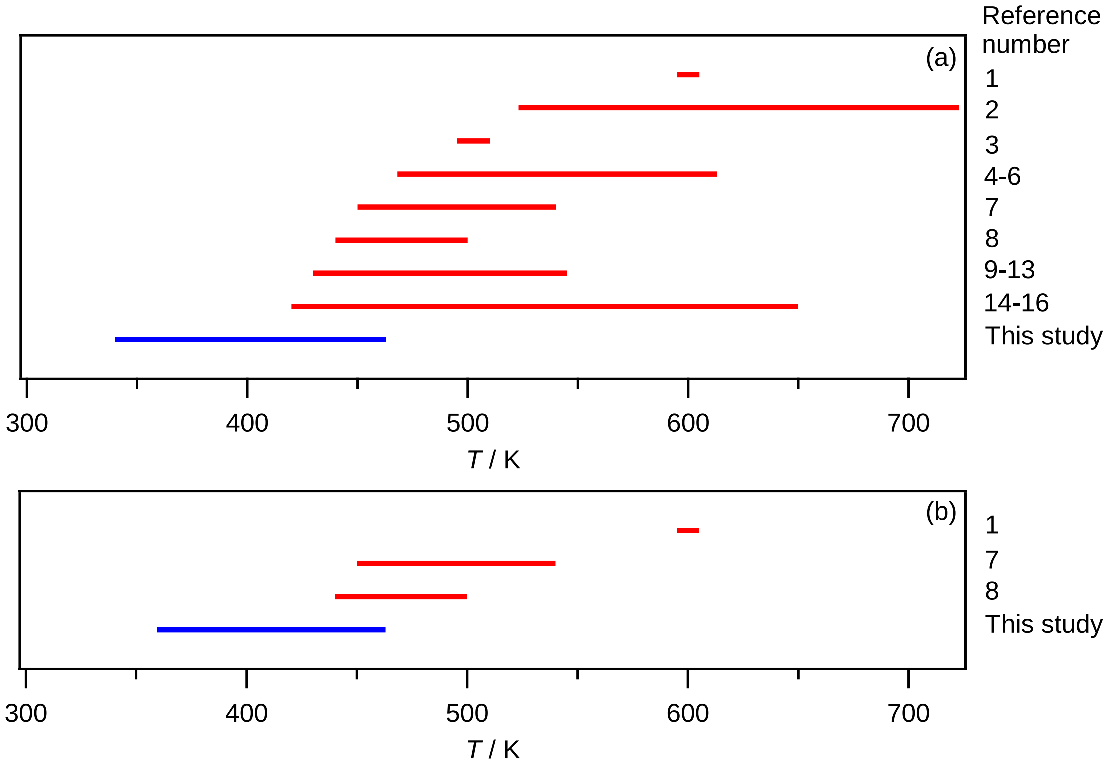

Figure S.1. Temperature of vapour phase measurements by different research groups (the corresponding author is listed on the right hand side). Previous publications are shown in red and this study is shown in blue. (a) Enthalpy of vaporisation at T, $\Delta_{vap}H_T$.[1-16] (b) Vapour pressure.[1,7,8]

Section 2. LOS mass spectrometer set-up

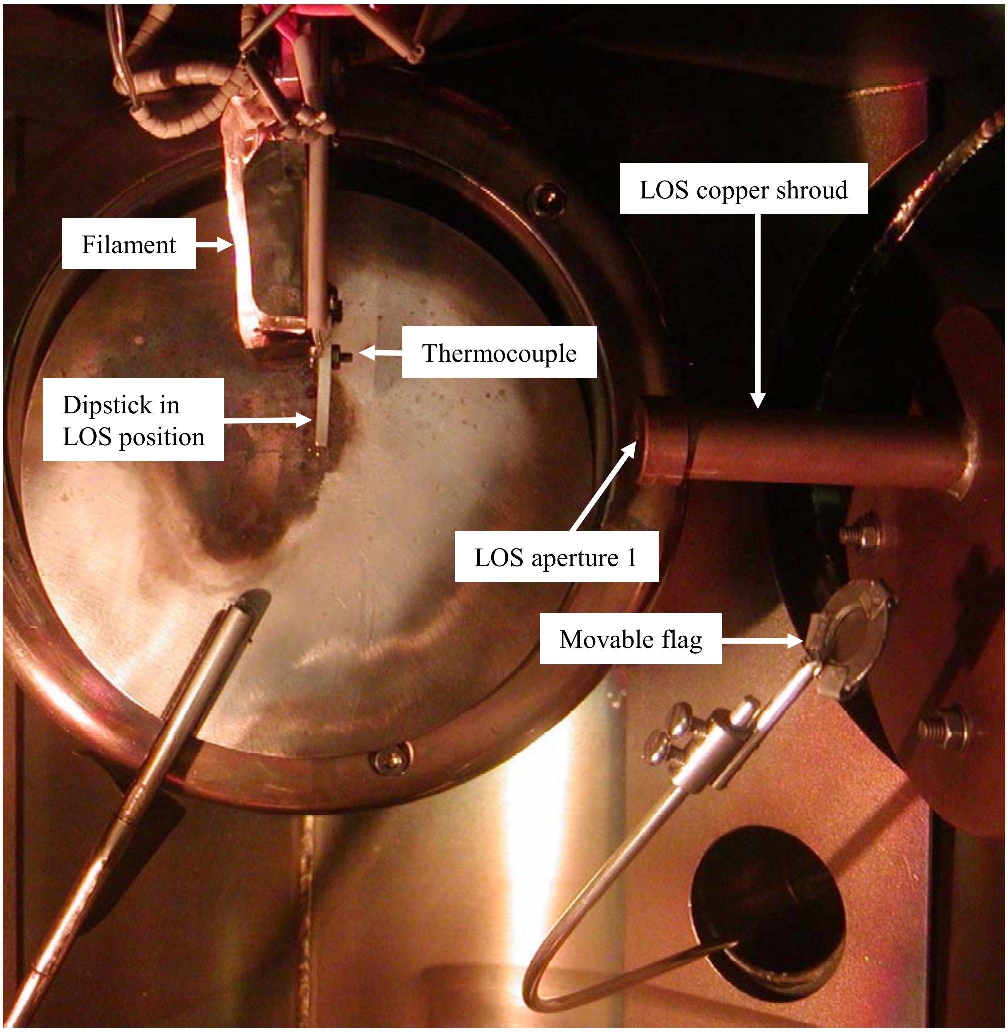

Figure S.2. Annotated photograph of the LOS mass spectrometer set-up. The sample heating filament was on when this photograph was taken.

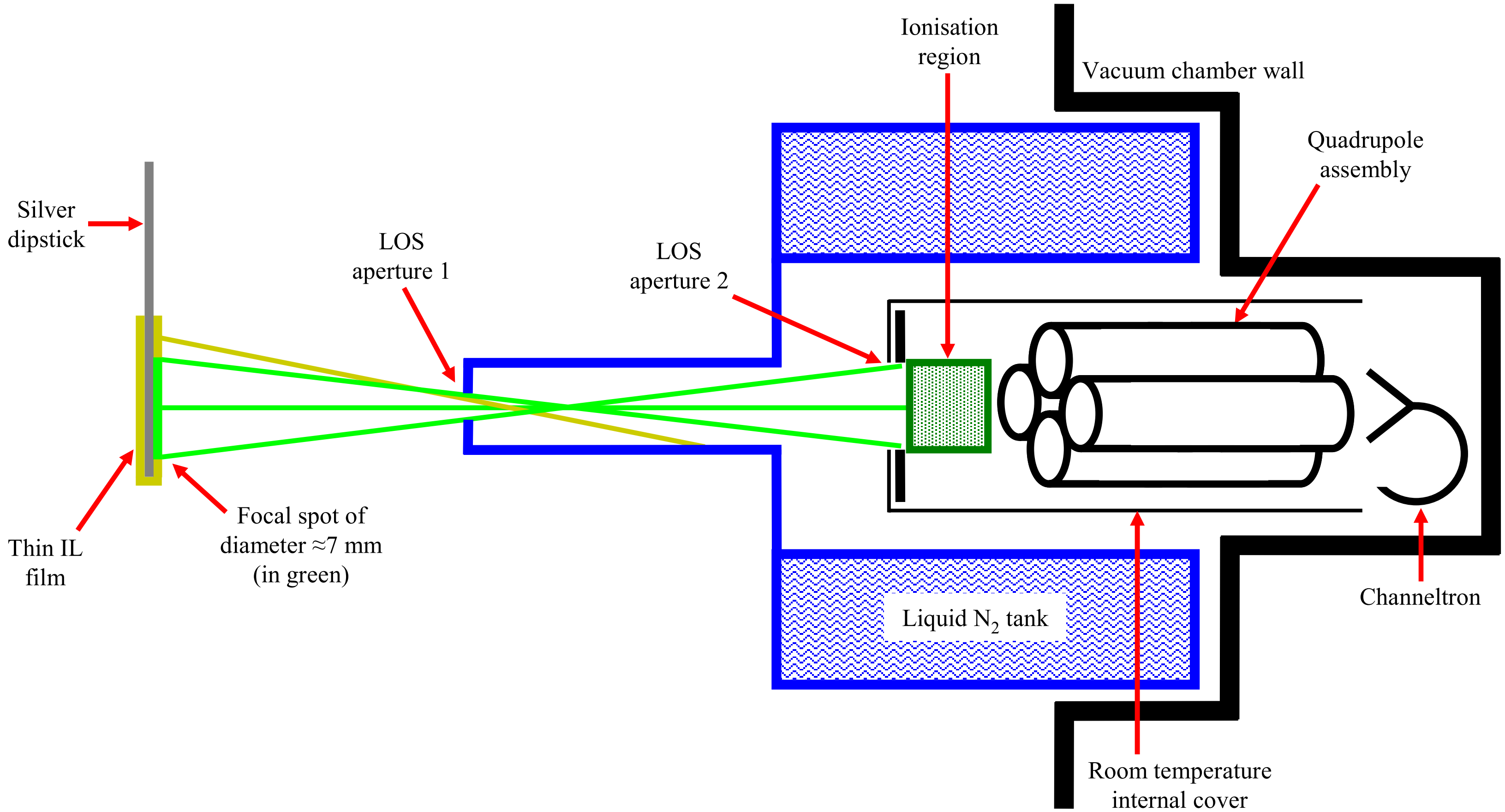

Figure S.3. Schematic of LOS mass spectrometer (not to scale). Two LOS apertures define a focal spot on the surface of the sample, diameter ≈7 mm, in LOS with the ionisation region. The green species are in the field of view of the ionisation region; the yellow species are not.

Section 3. Background subtraction for wide scan mass spectra

In mass spectrometry (MS) it is vital to employ a background subtraction to obtain a true spectrum of the vapour being investigated, in particular for quadrupole MS.[2] Conventional background subtraction involves subtracting an "off" mass spectrum from an "on" mass spectrum. The "on" spectrum contains both the vapour of interest and the background contaminants, and the "off" spectrum contains only the background contaminants. The "off" spectrum is often recorded at room temperature, prior to vaporisation of the vapour of interest. Contamination of a mass spectrometer has already been found to be a problem for MS of ionic liquids (ILs).[17]

For these experiments carried out using quadrupole MS there are four potential sources of ions. The first, and most important, source is ionisation of molecules that have vaporised directly from the IL sample on the dipstick to the ionisation region inside the mass spectrometer. The signal from this species is the signal that needs to be isolated from all other "contaminant" species. The probability of an electron-molecule collision inside the ionisation region, and hence ionisation, is relatively low.[2] Most vapour that enters the mass spectrometer will not be ionised on the first pass through the ionisation region. The IL vapour would not evaporate from the room temperature internal cover inside the mass spectrometer and consequently the IL vapour operated on an effective single pass regime.

The only exception to this single pass regime gives rise to the second source of ions. The IL vapour can potentially condense on parts of the mass spectrometer that are hotter than the internal cover; for example, the area surrounding the filament will be above room temperature. Depending upon the temperature of the surface, the IL will either re-evaporate as an intact neutral ion pair or thermally crack and evaporate as stable fragment species. Thermal cracking of the IL will give rise to signals from anionic species such as $[SO_2]^{+\bullet}$ for $[Tf_2N]^-$-containing ILs.

The third source of ions was ionisation of those molecules already present inside the mass spectrometer before desorption of the IL began; peaks from such species are referred to as mass spectrometer memory peaks. Examples of such ions include $[H_2O]^{+\bullet}$, $[SO_2]^{+\bullet}$, $[CF_3]^+$ and $[C_1Im]^{+\bullet}$. These species were likely to vaporise from the room temperature internal cover. Hence these contaminant species operated on a multiple pass regime, leading to a higher probability of detection compared to the IL vapour. Therefore the intensity of the contaminant species, relative to the intensity of the ions from the IL vapour, would be disproportionately large.

The fourth source of ions was those species that are not trapped by the LOS cryopump. These molecules enter the mass spectrometer from the main UHV chamber throughout the course of the experiment. Examples of such ions include $[H_2]^{+\bullet}$, $[CO]^{+\bullet}$, and $[CO_2]^{+\bullet}$.

The presence of these contaminant ions renders conventional background subtraction (*i.e.* recording an "off" background mass spectrum before the experiment has begun and subtracting from the "on" mass spectrum) redundant as the contaminant levels varied unpredictably throughout any given experiment. This situation led to subtracted spectra that contained significant amounts of ions that were not produced by ionisation of the IL vapour.

A flag, or blocking device, was used that could be placed into the LOS position between the dipstick and the ionisation region of the mass spectrometer. By recording mass spectra immediately before and after the flag was placed in the LOS position a far better background subtraction was achieved. The flag was placed in the LOS position between mass spectra, *i.e.* an "on" mass spectrum was taken with the flag not in place and then an "off" mass spectrum was taken with the flag in place. Each mass spectrum took approximately 60 seconds to record. Consequently there was a substantial time differential between the placing of the flag in the LOS position and recording of data points, particularly for higher *m/z* values.

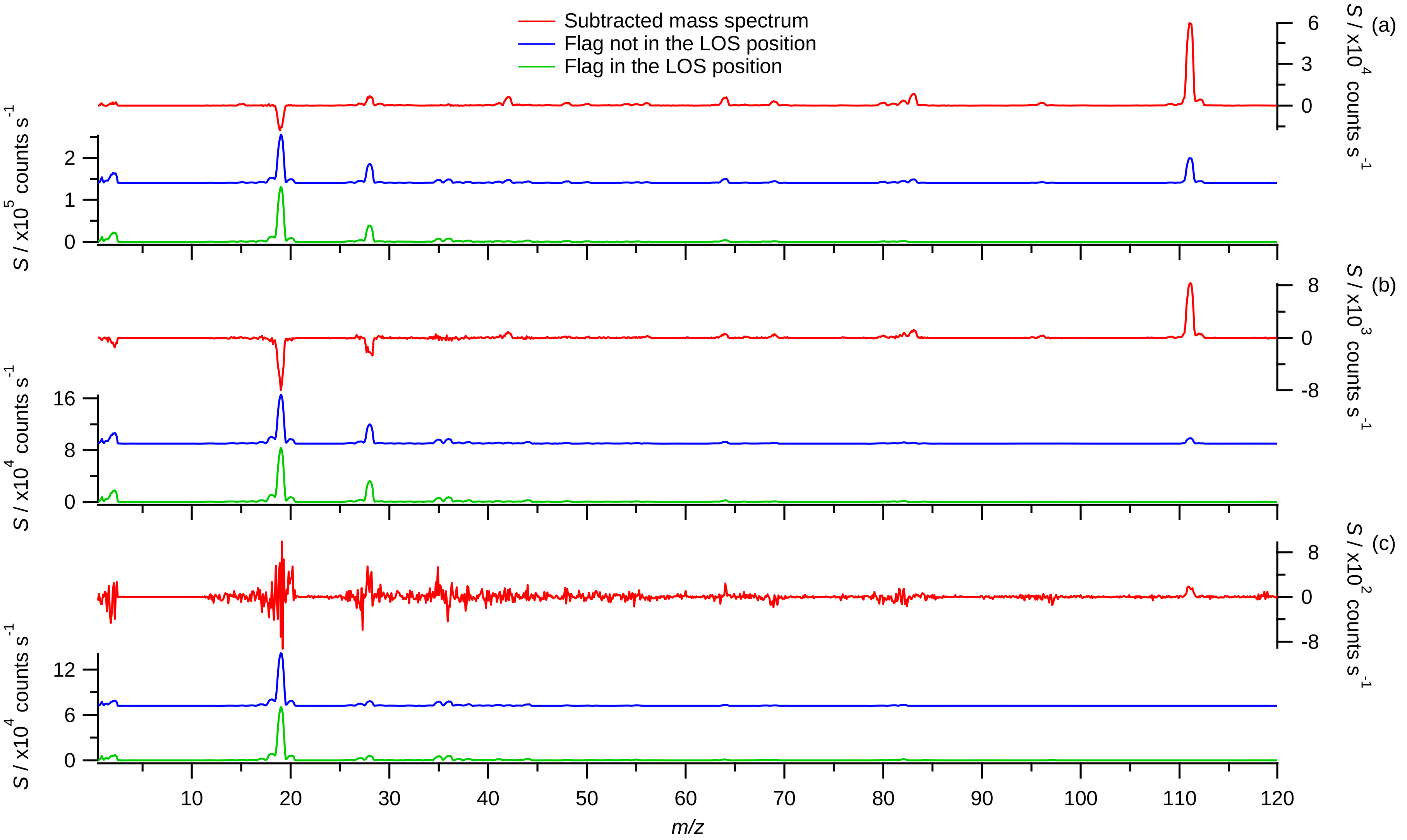

Figure S.4. LOS mass spectra intensity, *S*, versus mass-to-charge ratio, *m/z*, for [C_2C_1Im][Tf_2N] at (a) *T* = 439 K, (b) *T* = 414 K, (c) *T* = 373 K. The red traces are the subtracted spectra, the blue traces are with the flag not in the LOS position and the green traces are with the flag in the LOS position.

Section 4. Ionic liquid synthesis and characterisation

All reagents were purchased from Sigma-Aldrich and used as received, with exception of 1-methylimidazole, which was dried over CaH_2 and distilled prior to use. Routine diagnostic ^1H and ^{13}C NMR spectra were measured on a Bruker DPX-300 spectrometer at 300 and 75 MHz respectively. All NMR samples were prepared in DMSO-d_6. All ionic liquids used were analysed by ion chromatography (Dionex ICS-3000) before use; in all cases [Cl^-] was < 100 ppm. Prior to investigation in UHV, each IL sample was degassed on a glass Schlenk line at 10^{-2} mbar and 318–343 K for 18 hrs. Using distillation apparatus in a separate study, our group have observed that for [C_8C_1Im][Tf_2N] relatively small amounts of 1-methylimidazole, a starting material for the IL synthesis, have been detected as desorbing at ≈415-495 K and ≈1 × 10^{-3} Pa,[13] indicating that careful degassing at relatively low pressures is required for truly pure IL samples, which are of particular importance for vapour phase studies.

Section 5. Enthalpy of vaporisation

Table S.1. $\Delta_{vap}H_T$ and $\Delta_{vap}H_{298}$ values (in kJ mol^{-1}) and T values (in K). Both Luo *et al.*[3] and Seeberger *et al.*[1] gave $\Delta_{vap}H_T$ only; $\Delta_{vap}H_{298}$ was calculated here using $\Delta_l^gC_p$ = -100 J K^{-1} mol^{-1}. All $\Delta_{vap}H_{298}$ values have been rounded to zero decimal places. For $[C_3(C_1Im)_2][Tf_2N]$ a different $\Delta_l^gC_p$ value (-130 J K^{-1} mol^{-1}) was used to reflect the different vapour phase observed.[12]

Ionic Liquid	LOSMS[9-12]			Knudsen effusion[8]			Transpiration[7]			Microcalorimetry[16]			TGA[3]			TGA[1]			Photoionisation[5]		
	$\Delta_{vap}H_T$	$\Delta_{vap}H_{298}$	T	$\Delta_{vap}H_T$	$\Delta_{vap}H_{298}$	T	$\Delta_{vap}H_T$	$\Delta_{vap}H_{298}$	T	$\Delta_{vap}H_T$	$\Delta_{vap}H_{298}$	T	$\Delta_{vap}H_T$	$\Delta_{vap}H_{298}$	T	$\Delta_{vap}H_T$	$\Delta_{vap}H_{298}$	T	$\Delta_{vap}H_T$	$\Delta_{vap}H_{298}$	T
$[C_2C_1Im][Tf_2N]$	118	134	430	118.8	135	463.0	116.56	137	499.2	110.4	136	577.8	120.6	140	495.5						
$[C_3C_1Im][Tf_2N]$										121.0	147	577.8									
$[C_4C_1Im][Tf_2N]$	117	134	440	118.3	136	477.6				128.4	155	577.8	118.5	138	495.5	108	138	600			
$[C_5C_1Im][Tf_2N]$										134.3	162	577.8									
$[C_6C_1Im][Tf_2N]$	121	139	445	123.4	140	461.8				144.5	173	577.8	124.1	145	503.0						
$[C_7C_1Im][Tf_2N]$										151.4	180	577.8									
$[C_8C_1Im][Tf_2N]$	131	149	450	132.3	150	475.2				162.9	192	577.8	132.3	153	503.0						
$[C_{10}C_1Im][Tf_2N]$													134.0	155	510.0						
$[C_3C_1C_1Im][Tf_2N]$													130.0	151	503.0						
$[C_2C_1Im][Pf_2N]$													115.3	136	503.0						
$[C_4C_1Im][Pf_2N]$													114.4	135	503.0						
$[C_6C_1Im][Pf_2N]$													118.4	139	503.0						
$[C_8C_1Im][Pf_2N]$													125.0	145	499.3						
$[C_{10}C_1Im][Pf_2N]$													127.4	148	510.0						
$[C_3C_1C_1Im][Pf_2N]$													121.9	142	503.0						
$[C_8C_1Im][BF_4]$	137	162	520																		
$[C_8C_1Im][PF_6]$	143	169	530																		
$[C_8C_1Im][TfO]$	128	151	495																		
$[C_8C_1Im][N(CN)_2]$	141	162	520																		
$[C_2C_1Im][EtOSO_3]$	141	164	500																		
$[C_2C_1Im][BF_4]$	128	149	515																		
$[C_2C_1Im][SCN]$	133	151	490																		
$[C_4C_1Im][FeCl_4]$	150	170	510																		
$[C_4C_1Im][N(CN)_2]$							142.13	157	448.7										156	174	476
$[C_4C_1Pyrr][N(CN)_2]$	142	161	500																151	171	483
$[C_4C_1Pyrr][FAP]$	138	152	450																		
$[C_4C_1Pyrr][Tf_2N]$	136	152	470																167	195	598
$[C_6C_1Pyrr][Tf_2N]$	141	156	460																		
$[C_8C_1Pyrr][Tf_2N]$	145	161	470																		
$[C_4Py][BF_4]$	146	167	510																		
$[C_6Py][Tf_2N]$	139	152	440																		
$[C_3(C_1Im)_2][Tf_2N]$	158	190	545																		

The following equations were produced from the plots of ln(S_{111}) versus $1/T$. These equations were used to produce the lines in Figures 2 and 3.

For [C_2C_1Im][Tf_2N]:

$$S = 6.45\times10^{18}\exp(-1.18\times10^{5}/RT) \quad (1)$$

For [C_2C_1Im][$EtOSO_3$]:

$$S = 6.25\times10^{18}\exp(-1.35\times10^{5}/RT) \quad (2)$$

Converting E_a to $\Delta_{vap}H_T$

For zero order desorption occurring with a linear heating rate a plot of ln(S_{111}) against $1/T$ gives a gradient of $-E_a/R$. As evaporation occurs into a vacuum the expanding gas does no work and hence:

$$E_a = \Delta_{vap}U_{Tav} \quad (3)$$

where $\Delta_{vap}U_{Tav}$ is the change in internal energy for vaporisation at the average temperature for desorption, T_{av}. Enthalpy, H, is defined as:

$$H = U + pV \quad (4)$$
$$\Delta H = \Delta U + \Delta n_g RT \quad (5)$$
$$\Delta_{vap}H_{Tav} = \Delta_{vap}U_{Tav} + RT_{av} \quad (6)$$

where $pV = n_gRT$ and $n_g = +1$ for desorption of IL neutral ion pairs (NIPs).

To convert the molar enthalpy of vaporisation from T_{av} to 298 K the difference in heat capacity at constant pressure ($\Delta_l^gC_p = C_{p,g} - C_{p,l}$) between the IL in the vapour ($C_{p,g}$) and liquid ($C_{p,l}$) phases is required:

$$\Delta H = C_p\Delta T \text{ (at constant pressure)} \quad (7)$$
$$\Delta_{vap}H_{298} = \Delta_{vap}H_T + \Delta_l^gC_p(T_{av} - 298) \quad (8)$$

It is an assumption that $\Delta_{vap}H$ is constant over the relatively small temperature range (≈90 K in this work) for which fitting is carried out. This assumption is valid as the variation would be due to thermal effects, and these are negligible over small temperature ranges. The measured values available for $\Delta_l^gC_p$ are limited; estimates have been made using a combination of calorimetric data and statistical thermodynamics calculations.[7,8,16,18,19] Hence, $\Delta_l^gC_p$ is presently not determined directly from experimental data and therefore the values used cannot be verified. Paulechka *et al.* have also found $\Delta_l^gC_p$ values to be constant, within estimated uncertainties, in the range of temperatures from 298 K to 500 K.[19]

Table S.2. $\Delta_l^g C_p$ values used thus far for estimating $\Delta^g{}_l C_p$ for ILs.

$\Delta_l^g C_p$ / J K^{-1} mol^{-1}	T range / K	ILs studied	Reference
-94	430 - 545	Wide range of cations and anions	9-11
-100	463 - 475	$[C_nC_1Im][Tf_2N]$	8
-90.7 to -105.0	577.8	$[C_nC_1Im][Tf_2N]$	16
-100	449 - 538	$[C_2C_1Im][Tf_2N]$ $[C_4C_1Im][N(CN)_2]$	7
-130	545	$[C_3(C_1Im)_2][Tf_2N]$	12

Section 5. Impurity detection

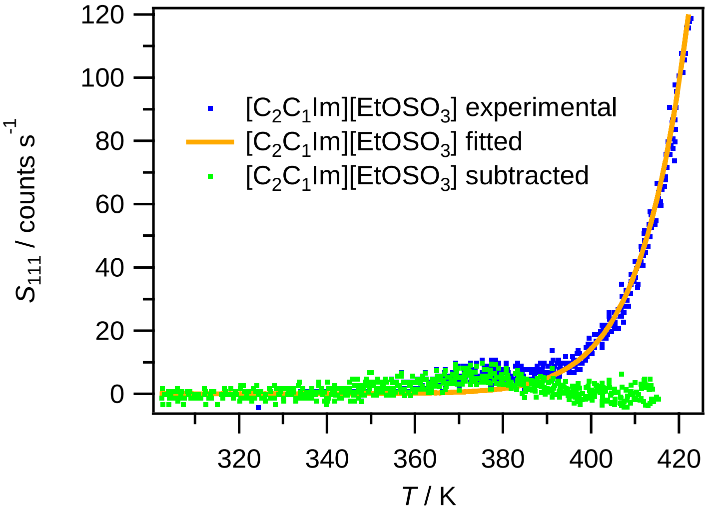

Figure S.5. LOS mass spectrum intensity versus temperature for $[C_2C_1Im][EtOSO_3]$ (blue dots), fitted trace (orange line) and the LOS mass spectrum intensity minus the fitted trace (green dots) showing the small but significant peak at 375 K.

Section 6. Measuring the vapour pressure

The mass of IL in the LOSMS region, *m*, was estimated by weighing the dipstick before and after an IL dip, $m = 16 \pm 3$ mg for both ILs. This weighing was carried out at atmospheric pressure for both ILs, leading to a small error due to viscosity differences caused by contaminants present at atmospheric pressure. The mass for both ILs was relatively similar, most likely due to their relatively similar viscosities (28.7 mPa s and 78.5 mPa s for $[C_2C_1Im][Tf_2N]$ and $[C_2C_1Im][EtOSO_3]$ at T = 303.5 K respectively[20]). The total amount of IL NIPs desorbed during the experiment, N_{tot}, is given by:

$$N_{tot} = N_A m/M \tag{9}$$

where N_A is Avogadro's number and M is the molar mass of one NIP of IL. The total number of NIPs desorbing per second at any particular temperature, $(dN/dt)_T$, is given by:

$$(dN/dt)_T = (S/S_{tot})N_A m/M \tag{10}$$

where S is the signal intensity of *m/z* 111 at a particular temperature T and S_{tot} is the area under the *m/z* 111 trace against time. For simplicity, an isotropic emission of NIPs is presumed (*i.e.* desorption is from a point source is therefore in spherical waves), even though the true distribution is expected to be a cosine distribution. This assumption introduces an error of approximately two times. In kinetic terms, the equilibrium vapour pressure occurs when the incident flux equals the desorption flux at the sample surface. We make the approximation that *m* radiates outwards from a centre point. To obtain the emission frequency, Z_{out}, of NIPs, s^{-1} m^{-2} at the surface of the sample, we divide dN/dT by the emitting area A_s:

$$Z_{out} = (S/S_{tot})N_A m/MA_s \tag{11}$$

A_S is measured using the dimensions of the dipstick (1.5 mm × 6 mm) and a dip depth of 12 mm. The collision frequency of a gas of pressure p with a wall is:

$$Z_{wall} = pN_A/(2\pi MRT)^{1/2} \tag{12}$$

For a liquid at equilibrium with its vapour pressure, p_{vp}, the emission frequency, Z_{out}, equals the collision frequency, Z_{wall}, at the surface, therefore at a given time or temperature in the TPD we can write:

$$(S/S_{tot})N_A m/MA_s = p_{vp}N_A/(2\pi MRT)^{1/2} \tag{13}$$

or

$$p_{vp} = (S/S_{tot})(m/A_s)(2\pi RT/M)^{1/2} \tag{14}$$

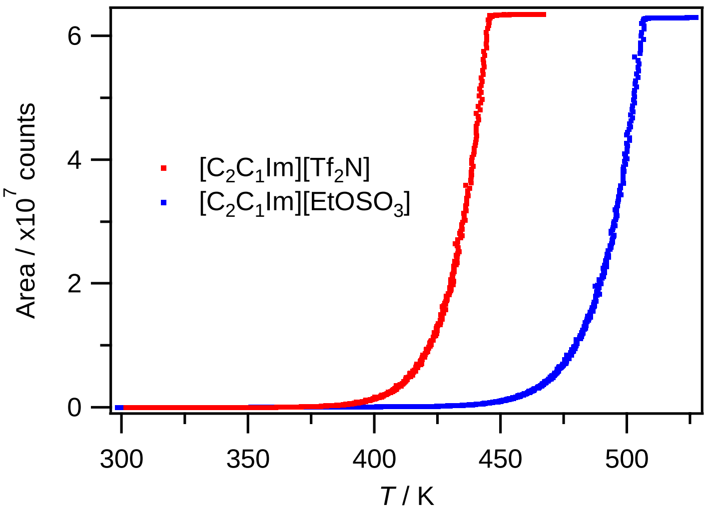

Figure S.6. Integral against time of the LOS mass spectrum intensity, S_{111}, versus temperature, T, for [C_2C_1Im][Tf_2N] (red trace) and [C_2C_1Im][$EtOSO_3$] (blue trace).

Table S.3. Calculating vapour pressure, p_{vp}, at temperature, T, for [C_2C_1Im][Tf_2N] and [C_2C_1Im][$EtOSO_3$].

Quantity	[C_2C_1Im][Tf_2N]	[C_2C_1Im][$EtOSO_3$]
M_{NIP} / kg mol^{-1}	0.391	0.236
S_{tot} / counts	6.3×10^7	6.2×10^7
T / K	425	490
S_T / counts s^{-1}	18500	24900
m / kg	2.5×10^{-5}	2.5×10^{-5}
N_{tot}	1.5×10^{-19}	2.5×10^{-19}
$(dN/dt)_T$ / s^{-1}	1.6×10^{16}	1.0×10^{16}
A_s / m^2	188×10^{-6}	188×10^{-6}
P_{vp} / Pa	9.3×10^{-3}	17.6×10^{-3}

The estimate the pressure exerted by an IL a given distance from the surface, the following derivation was used. For a point distance r from an infinite, planar, liquid surface, where the surface subtends an angle of 2π steradians (half a hemisphere) the pressure at that point will be the vapour pressure p_{vp}. On shrinking the emitting surface to a circular area A_s distance r along the perpendicular to an emitting surface, the angle subtended by the surface drops to Ω steradians. For large r compared to the emitting area ($r >> (A_s/\pi)^{1/2}$) the solid angle Ω is given by:

$$\Omega = 4\pi(A_s/4\pi r^2) = A_s/r^2 \qquad (15)$$

For simplicity, if we assume isotropic emission of NIPs rather than the cosine distribution expected for a surface, the pressure at position r will have dropped in proportion to the solid angle, $\Omega/2\pi$, giving:

$$p = p_{vp}(A_s/2\pi r^2) \qquad (16)$$

A_s is the area of emission which, considering the location of the ionisation gauge relative to the dipstick, is approximately $(12\times1.5+12\times6+1.5\times6)/2 = 50$ mm^2 = 5×10^{-5} m^2.

Table S.4. Vapour pressure, p_{vp}, at 400 K for the ionic liquids and a selection of metals.[21]

Compound	p_{vp} at 400 K / Pa
Mercury	140
Caesium	0.4
Rubidium	0.2
Potassium	2×10^{-2}
$[C_2C_1Im][Tf_2N]$	7×10^{-4}
Cadmium	3×10^{-4}
Sodium	2×10^{-4}
$[C_2C_1Im][EtOSO_3]$	6×10^{-6}
Zinc	1×10^{-6}
Magnesium	7×10^{-9}
Lithium	8×10^{-11}

References

[1] A. Seeberger, A. K. Andresen, and A. Jess, *Phys. Chem. Chem. Phys.*, 2009, **11**, 9375.
[2] J. H. Gross, *J. Am. Soc. Mass Spectrom.*, 2008, **19**, 1347.
[3] H. M. Luo, G. A. Baker, and S. Dai, *J. Phys. Chem. B*, 2008, **112**, 10077.
[4] D. Strasser, F. Goulay, M. S. Kelkar, E. J. Maginn, and S. R. Leone, *J. Phys. Chem. A*, 2007, **111**, 3191.
[5] S. D. Chambreau, G. L. Vaghjiani, A. To, C. Koh, D. Strasser, O. Kostko, and S. R. Leone, *J. Phys. Chem. B*, 2010, **114**, 1361.
[6] D. Strasser, F. Goulay, L. Belau, O. Kostko, C. Koh, S. D. Chambreau, G. L. Vaghjiani, M. Ahmed, and S. R. Leone, *J. Phys. Chem. A*, 2010, **114**, 879.
[7] V. N. Emel'yanenko, S. P. Verevkin, and A. Heintz, *J. Am. Chem. Soc.*, 2007, **129**, 3930.
[8] D. H. Zaitsau, G. J. Kabo, A. A. Strechan, Y. U. Paulechka, A. Tschersich, S. P. Verevkin, and A. Heintz, *J. Phys. Chem. A*, 2006, **110**, 7303.
[9] J. P. Armstrong, C. Hurst, R. G. Jones, P. Licence, K. R. J. Lovelock, C. J. Satterley, and I. J. Villar-Garcia, *Phys. Chem. Chem. Phys.*, 2007, **9**, 982.
[10] V. N. Emel'yanenko, S. P. Verevkin, A. Heintz, J. A. Corfield, A. Deyko, K. R. J. Lovelock, P. Licence, and R. G. Jones, *J. Phys. Chem. B*, 2008, **112**, 11734.
[11] A. Deyko, K. R. J. Lovelock, J. A. Corfield, A. W. Taylor, P. N. Gooden, I. J. Villar-Garcia, P. Licence, R. G. Jones, V. G. Krasovskiy, E. A. Chernikova, and L. M. Kustov, *Phys. Chem. Chem. Phys.*, 2009, **11**, 8544.
[12] K. R. J. Lovelock, A. Deyko, J. A. Corfield, P. N. Gooden, P. Licence, and R. G. Jones, *ChemPhysChem*, 2009, **10**, 337.
[13] A. W. Taylor, K. R. J. Lovelock, A. Deyko, P. Licence, and R. G. Jones, *Phys. Chem. Chem. Phys.*, 2010, **12**, 1772.
[14] M. J. Earle, J. M. S. S. Esperança, M. A. Gilea, J. N. Canongia Lopes, L. P. N. Rebelo, J. W. Magee, K. R. Seddon, and J. A. Widegren, *Nature*, 2006, **439**, 831.
[15] J. P. Leal, J. M. S. S. Esperança, M. E. M. da Piedade, J. N. Canongia Lopes, L. P. N. Rebelo, and K. R. Seddon, *J. Phys. Chem. A*, 2007, **111**, 6176.
[16] L. M. N. B. F. Santos, J. N. Canongia Lopes, J. A. P. Coutinho, J. M. S. S. Esperança, L. R. Gomes, I. M. Marrucho, and L. P. N. Rebelo, *J. Am. Chem. Soc.*, 2007, **129**, 284.
[17] G. P. Jackson and D. C. Duckworth, *Chem. Commun.*, 2004, 522.
[18] Y. U. Paulechka, D. H. Zaitsau, G. J. Kabo, and A. A. Strechan, *Thermochim. Acta*, 2005, **439**, 158.
[19] Y. U. Paulechka, G. J. Kabo, A. V. Blokhin, O. A. Vydrov, J. W. Magee, and M. Frenkel, *J. Chem. Eng. Data*, 2003, **48**, 457.
[20] J. Jacquemin, P. Husson, A. A. H. Pádua, and V. Majer, *Green Chem.*, 2006, **8**, 172.
[21] D. R. Lide, in 'Handbook Chemistry and Physics: a ready-reference book of chemical and physical data', Boca Raton, 2006.